Comprehensive evaluation of *MGMT* promotor methylation by nanopore sequencing

Skarphedinn Halldorsson [*1], Richard Nagymihaly[1], Areeba Patel [2], Petter Brandal[3,5], Ioannis Panagopoulos[3,5], Henning Leske [4,6], Marius Lund-Iversen[4], Felix Sahm [2], and Einar Vik-Mo [†1,7]

[1]Vilhelm Magnus Laboratory, Institute for Surgical Research, Department of Neurosurgery, Oslo University Hospital, Oslo, Norway

[2]Department of Neuropathology, University Hospital Heidelberg, Heidelberg, Germany

[3]Section for Cancer Cytogenetics, Institute for Cancer Genetics and Informatics, Oslo University Hospital

[4]Department of Pathology, Oslo University Hospital, Oslo, Norway.

[5]Department of Oncology, Oslo University Hospital, Oslo, Norway

[6]University of Oslo, Oslo, Norway

[7]Institute for Clinical Medicine, University of Oslo, Oslo, Norway

Abstract

Rationale: Methylation of the O6-methylguanine-DNA methyltransferase (*MGMT*) promoter region correlates with responsiveness to temozolomide treatment and overall survival in patients with glioblastoma, IDH wildtype (GBM) patients. However, there is currently no consensus on the optimal method to determine this methylation status. Conventional methods have limitations due to the dependence on bisulfite treatment and limited read length. Nanopore long-read sequencing offers methylation analysis of native DNA without the need for bisulfite treatment or amplification. Combined with recent advancements in targeting methods, nanopore sequencing can provide an accurate, comprehensive and cost-effective approach to *MGMT* promoter methylation analysis.

Methods: We analyzed all 98 CpG sites of the *MGMT* CpG island and 17 additional sites within the island shores in 148 CNS tumors using nanopore sequencing and compared the results to data obtained using pyrosequencing or methylation bead arrays. We used Oxford Nanopore Technologies (ONT) MinION flow cells to run single or barcoded (multiplex) assays,

*skarphedinn.halldorsson@rr-research.no
†einar.vik-mo@rr-research.no

following a CRISPR/Cas9 protocol, and included results from a nanopore adaptive sampling panel.

Results: Correlation between the four CpGs of *MGMT* analyzed by pyrosequencing and nanopore sequencing was 92%. Classification by the *MGMT* STP27 algorithm could also be recreated with data from nanopore sequencing. Unsupervised hierarchical clustering of nanopore sequencing data revealed a robust difference between unmethylated and methylated samples that could be used for patient classification, demonstrating comparable ability to predict patient survival.

Discussion: We found that nanopore sequencing of the *MGMT* promoter region is a valid method to determine the *MGMT* methylation status in GBM, providing high-confidence results within a few hours of sequencing. The extension of the analysis to all 98 CpGs of the *MGMT* CpG island provides a comprehensive picture of the methylation landscape of the *MGMT* promoter and identified potentially clinically relevant subgroups within both methylated and unmethylated cohorts. Further studies on the clinical implications of patient stratification by nanopore sequencing of the *MGMT* promoter are warranted.

Keywords: *MGMT* promoter methylation, Nanopore sequencing, CRISPR/Cas9, Glioblastoma

Introduction

Glioblastoma (GBM) is the most common and most aggressive primary malignant brain tumor in adults [Ostrom et al., 2020] with a median survival of about 15 months [Stupp et al., 2017]. Standard treatment for GBM involves surgical resection followed by a combination of radiation and chemotherapy. The frequently used chemotherapeutic drug temozolomide (TMZ) is an alkylating agent that induces DNA damage by methylation of O-6 guanidine residues in dividing cells, leading to DNA damage and apoptosis [Zhang et al., 2011]. Although often well tolerated, TMZ can cause a range of side effects and should therefore be limited to patients that may benefit from it and withheld from patients that most likely will only experience side effects without improvement in survival [Hegi and Ichimura, 2021]. The alkylating effects of TMZ are countered by the DNA repair protein O-6-methylguanine-DNA methyltransferase (MGMT). Methylation of the *MGMT* promoter is believed to silence its expression, thereby increasing sensitivity of GBM tumor cells to TMZ [Nakagawachi et al., 2003]. The presence of *MGMT* promoter methylation has been associated with increased survival in GBM patients treated with temozolomide and

radiation therapy [Hegi et al., 2019]. *MGMT* promoter methylation status is therefore an important factor for the management and treatment of GBM [Christmann et al., 2011].

Various methods are utilized to directly measure or estimate *MGMT* promoter methylation, including methylation-specific PCR, pyrosequencing, Sanger sequencing or methylation bead array [Johannessen et al., 2018]. All of these methods rely on bisulfite conversion of native tumor DNA prior to analysis and only include a subset of the 98 CpG sites in the CpG island of *MGMT* [Malley et al., 2011]. For example, the Qiagen *MGMT* pyrosequencing kit which is a common choice in the clinical setting, detects methylation on 4 CpG sites (76-79) in the *MGMT* promoter CpG island. In addition, there is neither a clear consensus on the best cut-off values for the classification of clinically relevant methylated or unmethylated samples, nor on the optimal method [Brandner et al., 2021]. In recent years, advances in sequencing technology have enabled more sensitive and accurate detection of DNA methylation. Nanopore sequencing, which uses a nanopore-based sensor to detect changes in electrical current as nucleic acids (DNA or RNA) pass through a pore, can detect epigenetic modifications, such as methylation, directly from the signal [Jain et al., 2016]. Due to the long-read nature of nanopore sequencing, it also affords methylation analysis of far longer sequences than methylation specific PCR, pyrosequencing or methylation bead array. Consequently, nanopore sequencing offers an overview of the methylation status of all CpGs of the *MGMT* CpG-island including the promoter region, using native genomic DNA without bisulfite conversion, which can be both time and cost efficient in a clinical setting [Laver et al., 2015]. Recently developed enrichment methods such as nanopore Cas9 targeted sequencing (nCATs) [Wongsurawat et al., 2020] and adaptive sampling (AS)[Payne et al., 2020] can be used to direct the sequencing effort to previously defined genomic regions. In this study, we compared the results of nanopore sequencing of the *MGMT* promoter region of 148 central nervous system (CNS) tumors, including 91 GBMs, with results obtained from standard diagnostic methods such as pyrosequencing or Illumina 850K bead array.

Materials and Methods

Patients and samples

Samples from three independent cohorts were included into this study; 1) Retrospective analysis of DNA from 68 CNS tumor samples provided by the Institute for Cancer Genetics and

Informatics, Oslo University Hospital that were screened for *MGMT* promoter methylation using the Qiagen® *MGMT* pyrosequencing kit (MGMT pyro kit). These samples are referred to as "Retrospective nCATs". 2) Retrospective analysis of 67 sequences generated as part of the Rapid-CNS adaptive sampling pipeline [Patel et al., 2022] analyzed by Illumina® methylation 850K bead array. These samples are referred to as "Rapid-CNS". 3) DNA extracted from 16 additional glioma biopsies from patients operated at Oslo University Hospital. A separate biopsy derived from paraffin-embedded tissue was analysed with the Qiagen® *MGMT* pyrosequencing kit at the Dept of Molecular Pathology. These samples are referred to as "Prospective nCATs". Supplementary Table 1 provides an overview of all samples used in this study.

In total, 153 samples from 148 patients were analyzed for *MGMT* promoter methylation status, including 91 GBM samples, 23 IDH-mutated glioma samples, and 12 meningioma samples. Figure 1b shows distribution of sample classification and predetermined methylation status. Two methods were used to enrich for the region of interest: CRISPR/Cas9 targeted sequencing of the *MGMT* promoter region [Wongsurawat et al., 2020] and adaptive sampling. Cas9 targeted sequencing was applied to 86 samples, 46 of which were run as single samples and 40 were run as multiplexed groups of five. 67 samples were previously analyzed as part of an adaptive sampling pipeline.

Sample preparation and Nanopore sequencing

Between 10 and 25 mg of fresh/frozen tissue were used to extract genomic DNA (Merck's GenElute™ Mammalian Genomic DNA Miniprep kit) following the manufacturer's protocol. Purity and concentration of DNA samples was determined using NanoDrop™ One and Qubit™ 4 Fluorometers (Thermo Fischer Scientific). Isolated DNA was stored at -20°C until analysis. Cas9 mediated targeted sequencing was performed with the Cas9 Sequencing Kit (Oxford Nanopore Technologies) according to the manufacturers protocol (version ENR 9084 v109 revR 04Dec2018). Briefly, Cas9 ribonucleoprotein complexes (RNPs) were created by mixing equimolar concentrations (100 µM) of crispr RNA (crRNA) and trans-activating elements (tracrRNA) to HiFi Cas9 enzyme (IDT). Dephosphorylated gDNA (2-5 µg) was cleaved and dA-tailed with Cas9 RNPs and Taq polymerase. Finally, sequencing adaptors were ligated to the cleaved fragments and the final DNA library was purified with AMPure XP beads (Beckman Coulter). Barcodes were applied to a number of samples to allow multiplexing of five samples based on an experimental protocol from Oxford Nanopore Technologies (UNPUBLISHED Cas9 Native Barcoding, version:

cas-native-barcoding-v1-revA). Purified DNA libraries were loaded onto R9.4.1. flow cells on MinION Mk1B or Mk1C devices and sequenced for 4-24 hours. Individual flow cells were flushed and re-used up to four times for single samples and twice for multiplexed samples. A minimum pore-count of 3000 was deemed sufficient for a single sample, 8000 for multiplexed samples. Raw fast5 sequences of all fragments mapping to the *MGMT* promoter in the Rapid-CNS data were provided for re-analysis.

Primers

All primers were purchased from Integrated DNA Technologies (Leuven, Belgium). Previously published primers were initially used to target the *MGMT* promoter [Wongsurawat et al., 2020], termed MGMT-left-1 (ATGAGGGGCCCACTAATTGA) and MGMT-right-1 (ACCTGAGTATAGCTCCGTAC), yielding a fragment of 2,522 bp. In order to increase cas9 efficiency and expand the size of the fragment, we added additional crRNA primers: MGMT-left-2 (GCCAACCACGTTAGAGACAATGG), MGMT-right-2 (GTACGGAGCTATACTCAGGT), MGMT-right3 (CTGGAATCGCATTCCAGTAGTGG) and MGMT-right-4 (ACTTCGCAAGCATCACAGGTAGG) resulting in a fragment of 4,800 bp.

Data analysis

Raw sequences were base-called, methylation called and mapped (hg19, chromosome 10) using the Megalodon toolbox (version 2.5.0 built on guppy version 6.2.7) from Oxford Nanopore Technologies (https://github.com/nanoporetech/megalodon). Methylation percentages of individual CpG sites were compiled using custom scripts in R. Samples with sequence coverage below 3 were removed from analysis. All statistical analyses were performed in R (version 4.2.1). The source code and data to reproduce all analyses and figures from this manuscript is available at https://github.com/SkabbiVML/MGMT_R.

Results

Data acquisition

Sequence depth of the *MGMT* promoter region in the samples varied based on method, sequencing time as well as DNA and flow-cell quality. Single sample runs produced on average

more sequences in the region of interest (mean = 92.1, median = 33) than barcoded runs (mean = 17.2, median = 12) and adaptive sampling (mean = 18.7, median = 15) (Supplementary Figure 1c). No bias in sequencing depth was observed between methylated and unmethylated samples across Cas9 targeted samples, either single or multiplexed. However, a slight but statistically significant difference in sequence depth was observed between methylated (mean = 23.6, median = 21) and unmethylated (mean = 16.5, median = 15) samples analyzed by adaptive sampling (p=0.021).

Nanopore Sequencing versus Pyrosequencing of the *MGMT* Promoter

A subset of our samples ("Retrospective nCATs", n=68) were analyzed using the Qiagen® *MGMT* pyrosequencing kit (MGMT pyro kit)), which specifically measures methylation on CpGs 76-79 of *MGMT*. To directly compare the results of nanopore sequencing and the *MGMT* pyro kit, we extracted methylation results for CpGs 76-79 from the nanopore data and compared them to methylation values obtained by the *MGMT* Pyro kit (Figure 2). Correlation between the methylation values of each overlapping CpG site between nanopore and pyrosequencing ranged from 0.78 to 0.88 (Figure 2a). Results from the *MGMT* pyro kit are typically returned as an average methylation percentage of all four CpGs for decision making. When results of nanopore sequencing and the *MGMT* pyro kit are averaged across all four CpG sites, correlation increased to 0.92 (Figure 2b).

We have previously established an average methylation level of $\geq$ 10% to be methylated, using the *MGMT* pyro kit [Johannessen et al., 2018, Håvik et al., 2012]. To compare classification results of nanopore sequencing and the *MGMT* pyro kit, a 10% average methylation threshold of CpGs 76-79 was applied to the nanopore data to re-classify *MGMT* methylated versus unmethylated samples (Figure 2c). A 91% concordance rate was observed between the two methods (62 of 68 samples were concordant) (Figure 2d). Notably, discordant results between nanopore sequencing and the *MGMT* pyro kit were in all cases classified as methylated by nanopore sequencing but unmethylated by pyrosequencing. No significant difference in sequencing depth was observed between concordant (mean = 26.2, median = 19) and discordant (mean = 17.5, median = 11.5) samples (p=0.465).

Nanopore sequencing versus STP27 and cumulative number of methylated CpG sites

Illumina® Human Methylation BeadChips (HM-27K, HM-450K, and HM-850K) are microarray-based platforms used to investigate DNA methylation patterns in human tumor samples. These platforms only cover a fraction of the approximately 30 million CpG sites in the human genome. To predict the clinically relevant methylation status of the *MGMT* promoter, a regression model, *MGMT STP-27*, has been developed. This model uses the methylation status of two array probes, cg12434587 (CpG 31) and cg12981137 (CpG 84), as reported by Bady *et al.* [Bady et al., 2012, Bady et al., 2016].

The samples from the Rapid-CNS study (n=67) were analyzed by Illumina® HM-850K EPIC array in addition to nanopore sequencing and the ground truth methylation status was derived from the *MGMT* STP-27 classifier. To compare nanopore sequencing results to the *MGMT* STP-27 classifier results, the methylation level of the two CpG sites represented in the *MGMT* STP-27 algorithm were extracted and the methylation percentage values were plotted against each other (Figure 3a). Methylated and unmethylated samples of the Rapid-CNS cohort could be separated with 95% accuracy (64 of 67) by an average methylation threshold of 12.5% of CpGs 31 and 84 (Figure 3b and Figure 3c).

Both the *MGMT* pyro kit and the *MGMT* STP-27 classifier rely on a very limited number of CpG sites to infer the clinically relevant methylation status of the whole *MGMT* promoter region. Recently, Siller *et al.* proposed a method for GBM patient stratification by counting individually methylated CpG sites within the second differentially methylated region (DMR2) of the CpG island of *MGMT* using Sanger bisulfite sequencing [Siller et al., 2021]. To emulate this approach we binarized the data for 25 CpG sites in DMR2 by applying a methylation cut-off of 10% to each site ($\geq$ 10% methylation = methylated, < 10% methylation = unmethylated). A near complete separation of methylated and unmethylated samples, according to their previously determined status, was observed when a cut-off threshold of $\geq$ 15 methylated CpG sites was applied (Figure 4a). Finally, we calculated the average methylation of the 117 CpG sites included and compared the average methylation to their previously determined status (Figure 4b). An average methylation threshold of 26% correctly separated methylated and unmethylated samples in 126 of the 128 samples.

Unsupervised clustering of CNS tumors based on nanopore sequencing

To investigate the impact of methylation at CpG sites including those not covered by the above-referenced methods, we performed hierarchical clustering of 98 CpG sites of the CpG island and included 7 CpGs upstream and 11 CpGs downstream. Unsupervised hierarchical clustering using Ward's method reveals two main clusters that largely correspond to the classification into methylated and unmethylated samples by pyrosequencing or methylation bead array (Figure 5a). Unmethylated samples exhibited low methylation levels throughout the CpG island, except for the first 5 CpG sites, which were often methylated. In contrast, methylated samples showed a larger gradient of methylation, with higher levels of methylation towards either end of the CpG island. The average methylation percentage of each CpG site in methylated and unmethylated samples (Figure 5b) revealed the biggest differences in methylation levels to occur at CpGs 6 through 15 and 71 through 90. Welch's two sided t-tests between methylated and unmethylated samples were performed at every CpG site and the results adjusted for multiple testing (Bonferroni method). Figure 5c shows the adjusted p-values for every site in the *MGMT* CpG island and its upstream and downstream shores. Interestingly, the lowest p-values were observed at CpG sites 3 through 13 (excluding CpG 6) which are far upstream of DMR1 and DMR2. Furthermore, 19 CpG sites were found to have lower p-values when comparing methylated and unmethylated samples than the CpG sites included in the *MGMT* pyro kit (CpGs 76-79) Figure 5c.

Unsupervised hierarchical clustering of all samples based on nanopore sequencing categorized five samples previously classified as methylated with otherwise unmethylated samples and one unmethylated sample with otherwise methylated samples (Figure 5a). This pattern of separation is also evident when unsupervised clustering was performed on GBM samples only (Figure 6a). In addition to the separation of samples into clusters that largely match the predetermined methylation status, k-means clustering indicated separation of samples within the methylated cluster (Figure 6d). Of the 22 samples that clustered with methylated samples, 9 specimen fell into a cluster that could be described as "very high methylation". The functional significance of these clusters remains to be determined.

Survival Analysis of GBM patients based on nanopore sequencing

While nanopore methylation profiles were often in agreement with bisulfite sequencing methods, discrepancies were also observed (Figure 5a). Therefore, we investigated whether cluster-

ing by nanopore sequencing was as effective in predicting patient survival as the MGMT pyro kit. We performed survival analysis on 25 GBM, IDH wildtype patients (11 females, average age 58.4 years and 14 males, average age 62.7 years) treated at Oslo University hospital by surgery followed by radiotherapy combined with concomitant and adjuvant temozolomide. Biopsies were analyzed by both MGMT pyro kit and cas9-targeted nanopore sequencing (Table 1). Patients were classified as methylated or unmethylated based on the 10% cut-off value by the MGMT pyro kit or placement within the two major clusters by hierarchical clustering of nanopore sequencing data Figure 6a.

Kaplan-Meier survival analysis of patients based on pyrosequencing showed significantly longer overall survival in patients classified as methylated compared to patients classified as unmethylated (Figure 6b, 22.0 vs. 12.0 months, p=0.0078). When patients were classified according to unsupervised clustering of nanopore sequencing data, significantly longer survival was observed in "Cluster 2" patients compared to "Cluster 1" patients (Figure 6c, 22.5 vs. 12.0 months, p=0.0039). Clusters 1 and 2 largely represent unmethylated and methylated patients, respectively, with some exceptions.

Discussion

Ever since *MGMT* promoter methylation was discovered as a prognostic marker for over-all and progression-free survival in GBM [Hegi et al., 2005, Dovek et al., 2019], there has been an ongoing debate regarding the optimal method and optimal cut-off to determine clinically significant methylation of the *MGMT* promoter (Supplementary Table 2). Methylation-specific PCR, pyrosequencing and methylation bead arrays are commonly used but when these methods have been directly compared, results have been discordant in up to a third of cases [Tierling et al., 2022, Håvik et al., 2012, Johannessen et al., 2018]. This is likely due to lack of consensus between CpG sites queried by different methods and different cut-offs applied. A recent meta-analysis including 32 cohorts and 3474 patients could not draw strong conclusions of the optimal CpG sites to query and optimal cut-off to apply [Brandner et al., 2021]. This underlines the need for method validation by every institution on their own patient cohort. Considerable effort has been put into finding a minimal set of CpG sites within the *MGMT* CpG island that can best predict *MGMT* expression and/or patient survival [Bady et al., 2016, Johannessen et al., 2018, Brigliadori et al., 2016, Radke et al., 2019, Siller et al., 2021]. This is partially due to the neces-

sity to provide simplified assays that fit the short-read framework of bisulfite sequencing techniques. Most, if not all, clinically established methods of *MGMT* methylation classification, such as methylation specific PCR, quantitative methylation specific PCR, MGMT pyro kit or the *MGMT* SPT27 classifier, rely on the methylation status of very limited number of CpG sites to predict the methylation status of the whole promoter. Although these assays have been shown to largely agree on highly methylated or completely unmethylated samples, they are less reliable when it comes to moderately methylated or 'grey-zone' patients [Torre et al., 2022].

Analysis of *MGMT* promoter methylation by nanopore sequencing has several advantages over conventional techniques. First, nanopore sequencing can detect epigenetic modifications on native DNA, thereby circumventing the need for bisulfite treatment. This saves time and reduces the potential risk of bias introduced by bisulfite treatment that has been shown to underrepresent densely hydroxymethylated (5hmC) regions [Huang et al., 2010]. This may partly explain the higher estimation of methylation by nanopore sequencing when compared to the *MGMT* pyro kit, particularly in cases previously classified as low methylation samples. Using native DNA without manipulation or amplification also reduces the risk of bias between sequencing data generated by different laboratories. Secondly, the long-read nature of nanopore sequencing offers a complete overview of methylation in the *MGMT* CpG island and can be extended in either direction to include the shores and shelves of the CpG island. Regions outside the DMR2 are neglected by most common assays but have been shown to discriminate the methylation status of GBMs [Tierling et al., 2022]. Third, the flexibility of nanopore sequencing makes it possible to incorporate *MGMT* methylation analysis to assays such as whole genome sequencing, exome sequencing, *in silico* enrichment (adaptive sampling) or cas9 targeted enrichment, either as single samples or multiplexed. Finally, the up-front cost of nanopore sequencing is low compared to other sequencing techniques and can be established by smaller laboratories or clinics.

In this study we analyzed 148 CNS tumors using targeted nanopore sequencing and compared the results to those acquired by pyrosequencing and methylation bead arrays. We found a 92% correlation between nanopore sequencing of the four CpG sites typically analyzed by pyrosequencing, with discrepant cases of being from samples with low methylation levels that were sometimes overestimated with nanopore sequencing compared to pyrosequencing. Nanopore sequencing was also able to recreate the results of the *MGMT* STP-27 classifier and emulate

results that were generated by Sanger bisulfite sequencing. In addition, nanopore sequencing allowed expansion of the area of analysis including additional 94 CpGs of the *MGMT* CpG island as previously proposed to be critical for MGMT expression [Nakagawachi et al., 2003]. Unsupervised hierarchical clustering of samples based on nanopore methylation data including 115 CpGs in and adjacent to the *MGMT* promoter showed clear separation of methylated and unmethylated samples. Finally, we showed that patient survival prediction based on methylation classification by nanopore sequencing of the *MGMT* promoter was at least comparable to pyrosequencing. To the best of our knowledge, this is the first study to examine all 98 CpG sites within the *MGMT* CpG island, along with its shores in multiple patient biopsies by nanopore sequencing.

The results presented here demonstrate that nanopore sequencing of the *MGMT* promoter region can largely recreate the results of conventional bisulfite dependant methods while providing additional data on epigenetic regulation of the *MGMT* gene and may provide novel criteria for patient stratification. Although the sample size is small, our results suggest that classifying patients via nanopore sequencing is as reliable as classification with other conventionally used methods such as the MGMT pyro kit, Sanger sequencing and methylation bead arrays. Unsupervised hierarchical clustering of glioblastoma samples based on nanopore sequencing indicates the presence of one or more sub-groups within the previously defined methylated samples. These groups are defined both by extent and level of methylation. Further studies and larger patient cohorts are needed to elucidate the functional implications of these sub-groups.

The study is not without limitations. Although 148 biopsies were included for the evaluation of nanopore sequencing as a method to analyse *MGMT* CpG island methylation, only 91 samples were from diagnosed GBM patients and survival data from primary GBM patients was only available for 25 patients. This limited our ability to evaluate survival beyond the major groups. Our data do not include estimation of tumor-cell content in the biopsies and do not take into account the possibilities of heterogeneous regions of *MGMT* promoter methylation that has previously been shown to affect some gliomas [Wenger et al., 2019]. Nanopore sequencing of the *MGMT* CpG island revealed single cases, where methylation status of *MGMT* was discordant with the results from the other tested conventional methods. However, such discrepancy reveals uncertainties in the currently used classification of the *MGMT* methylation status and justifies further studies. In particular, the high level of granularity in nanopore data provides a

basis to improve classification in such border-line samples in the future.

We conclude that methylation status evaluation by nanopore sequencing of the *MGMT* promoter region is comparable to standard methods such as pyrosequencing while providing considerable additional information. This is true for both cas9 targeted sequencing of the *MGMT* CpG island and inclusion of the *MGMT* promoter into an adaptive sequencing panel. Distinct subgroups within methylated samples were observed via nanopore sequencing although any difference in patient outcome between these clusters has yet to be determined.

Funding

This project was funded by the Norwegian research council grant number XXXXXXXXX

Acknowledgements

The authors would like to thank the patients who participated in this study and their families. We also thank Dr. Thidathip Wongsurawat for sharing her knowledge on Cas9 targeted sequencing and primer sequences.

Tables

Table 1: Patients used in survival analysis

Age	Sex	Diagnosis	IDH	Resection	Treatment	OS (months)	Status	*MGMT* Status (Pyro)	Nanopore cluster
66	F	GBM	Neg	GTR	Stupp	14.99	Dead	Unmethylated	1
78	M	GBM	Neg	GTR	Stupp	5.19	Dead	Methylated	2
58	M	GBM	Neg	STR	Stupp	24.5	Dead	Methylated	2
57	F	GBM	Neg	STR	Stupp	28.77	Dead	Methylated	2
73	M	GBM	Neg	STR	Stupp	20.91	Dead	Unmethylated	1
77	M	GBM	Neg	STR	Stupp	11.97	Dead	Unmethylated	1
60	M	GBM	Neg	GTR	Stupp	29.26	Dead	Methylated	2
65	M	GBM	Neg	STR	Stupp	29.69	Dead	Methylated	2
62	F	GBM	Neg	STR	Stupp	6.9	Dead	Unmethylated	1
64	M	GBM	Neg	STR	Stupp	25.48	Dead	Methylated	2
58	M	GBM	Neg	STR	Stupp	21.6	Dead	Methylated	2
58	M	GBM	Neg	STR	Stupp	11.44	Dead	Unmethylated	1
72	F	GBM	Neg	STR	Stupp	21.21	Dead	Methylated	2
58	F	GBM	Neg	STR	Stupp	13.61	Dead	Methylated	2
66	M	GBM	Neg	STR	Stupp	21.96	Dead	Methylated	2
51	M	GBM	Neg	GTR	Stupp	12.85	Dead	Methylated	2
64	F	GBM	Neg	STR	Stupp	8.3	Dead	Methylated	1
52	F	GBM	Neg	STR	Stupp	23	Dead	Methylated	2
66	F	GBM	Neg	STR	Stupp	13.6	Dead	Methylated	2
49	M	GBM	Neg	GTR	Stupp	9.4	Dead	Unmethylated	1
46	F	GBM	Neg	GTR	Stupp	14.31	Alive	Methylated	2
60	F	GBM	Neg	GTR	Stupp	14.08	Alive	Methylated	1
55	M	GBM	Neg	GTR	Stupp	15.16	Alive	Unmethylated	2
66	M	GBM	Neg	GTR	Stupp	14.47	Alive	Methylated	2
39	F	GBM	Neg	GTR	Stupp	13.78	Alive	Methylated	1

Figures

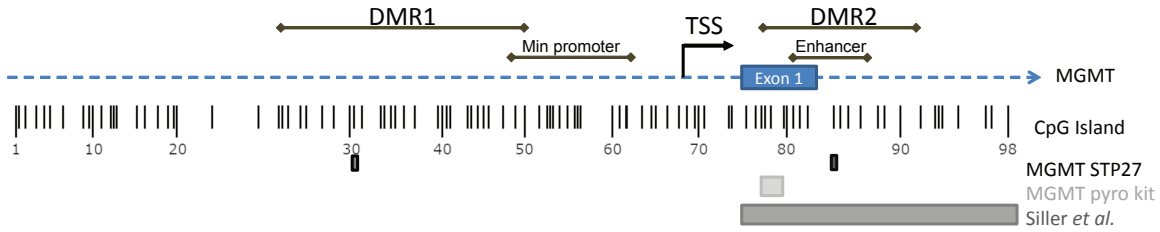

(a)

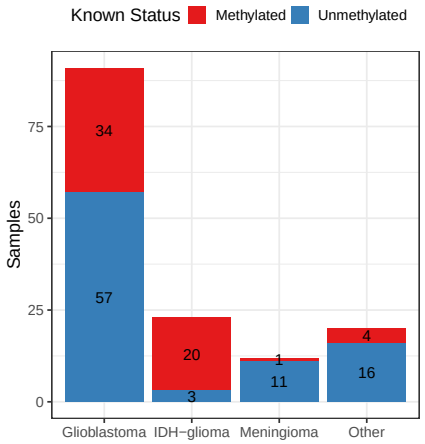

(b)

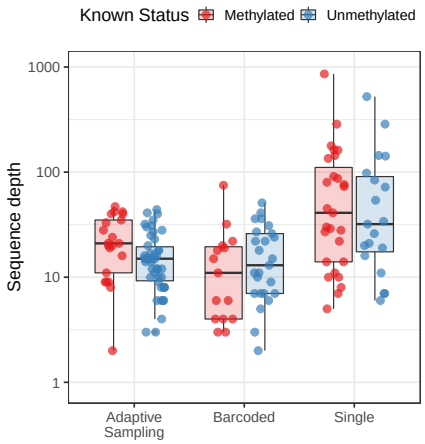

(c)

Figure 1: (a) Schematic overview of the 98 CpG sites of the *MGMT* promoter CpG island with relevant functional areas includin the transcription start site (TSS), minimal promoter and enhancer as defined by Harris *et al.* [Harris et al., 1991, Harris et al., 1994] as well as the differentially methylated regions (DMR) one and two as described by Malley *et al.* [Malley et al., 2011]. The two CpG sites used by the *MGMT* STP27 classifier [Bady et al., 2012], the four CpG sites included in the Qiagen® *MGMT* pyrosequencing kit and the 25 CpG sites suggested by Siller *et al.* [Siller et al., 2021] are shown below. (b) Distribution of diagnosis and known methylation status of the sample cohort. (c) Sequencing depth on the *MGMT* promoter region of methylated and unmethylated samples by method of acquisition (Adaptive sampling, multiplexed nCats, single sample nCats).

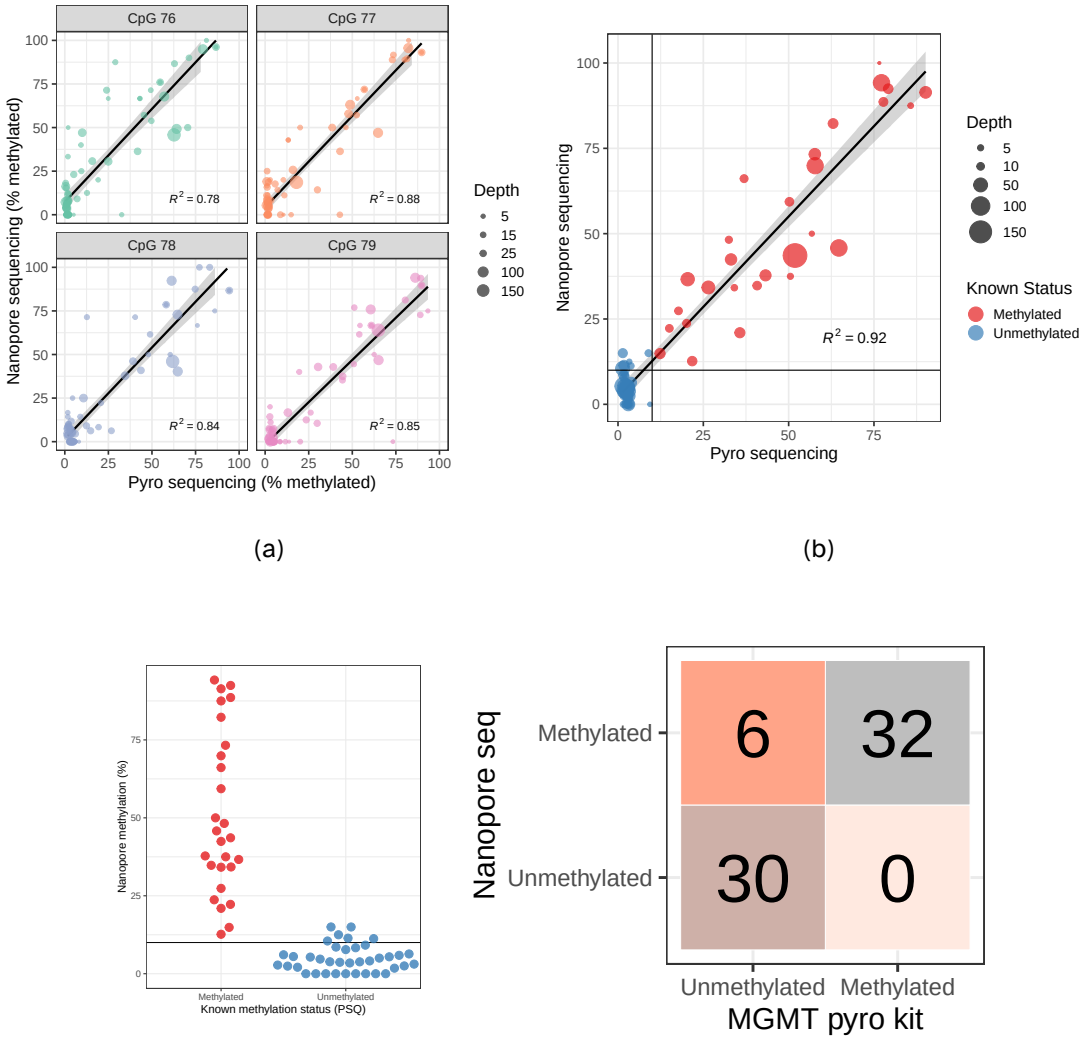

Figure 2: Comparison of nanopore sequencing and Qiagen® MGMT pyro kit of CpGs 76-79 in the *MGMT* CpG island. Results show per-site methylation percentage of each CpG (a) or average values of the 4 CpG sites analyzed by the MGMT pyro kit (b). Black horizontal and vertical lines mark a 10 % cut-off value between methylated and unmethylated samples. (c) Comparison of pyrosequencing classification into methylated versus unmethylated based on a 10% average methylation threshold of CpGs 76-79 in the *MGMT* promoter. The Y-axis represents average methylation percentage of the same four CpG sites based on nanopore sequencing. (d) Confusion matrix showing the concordance of classification via MGMT pyro kit and classification by average methylation of CpGs 76-79 as determined by nanopore sequencing based on a 10% methylated cut-off value.

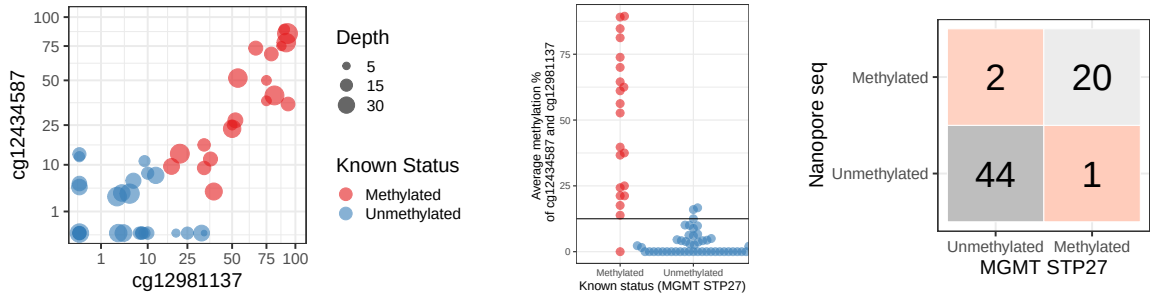

(a) (b) (c)

Figure 3: Comparison of nanopore sequencing results for CpG sites 31 and 84 in the *MGMT* CpG island to the *MGMT* STP27 classifier. (a) Methylation percentage of CpGs 31 and 84 for all samples in the Rapid-CNS cohort. Known status of these samples was derived from the STP27 classifier. (b) Average methylation of CpGs 31 and 84 plotted against the known methylation status. Horizontal line represents an average methylation percentage of 12.5%. (c) Confusion matrix showing concordance of the *MGMT* STP27 classifier and classification based on average methylation of CpGs 31 and 84 as determined by nanopore sequencing.

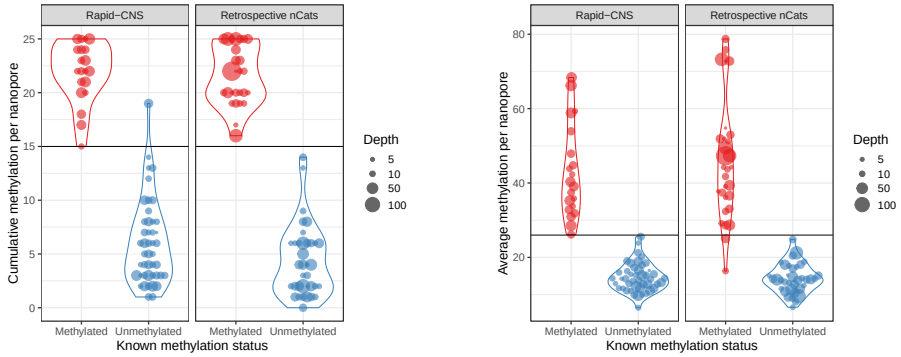

(a) (b)

Figure 4: (a) Comparison of cumulative methylation of the CpGs 74 -98 in the *MGMT* promoter region based on nanopore methylation and known status of samples, as proposed by [Siller et al., 2021]. (b) Comparison of average methylation percentage by nanopore sequencing of all CpG sites in the *MGMT* CpG island to known status. Known status of "Retrospective nCATs" samples derived by the *MGMT* pyro kit, known status of "Rapid-CNS" samples derived from methylation bead array (MGMT STP-27 classifier).

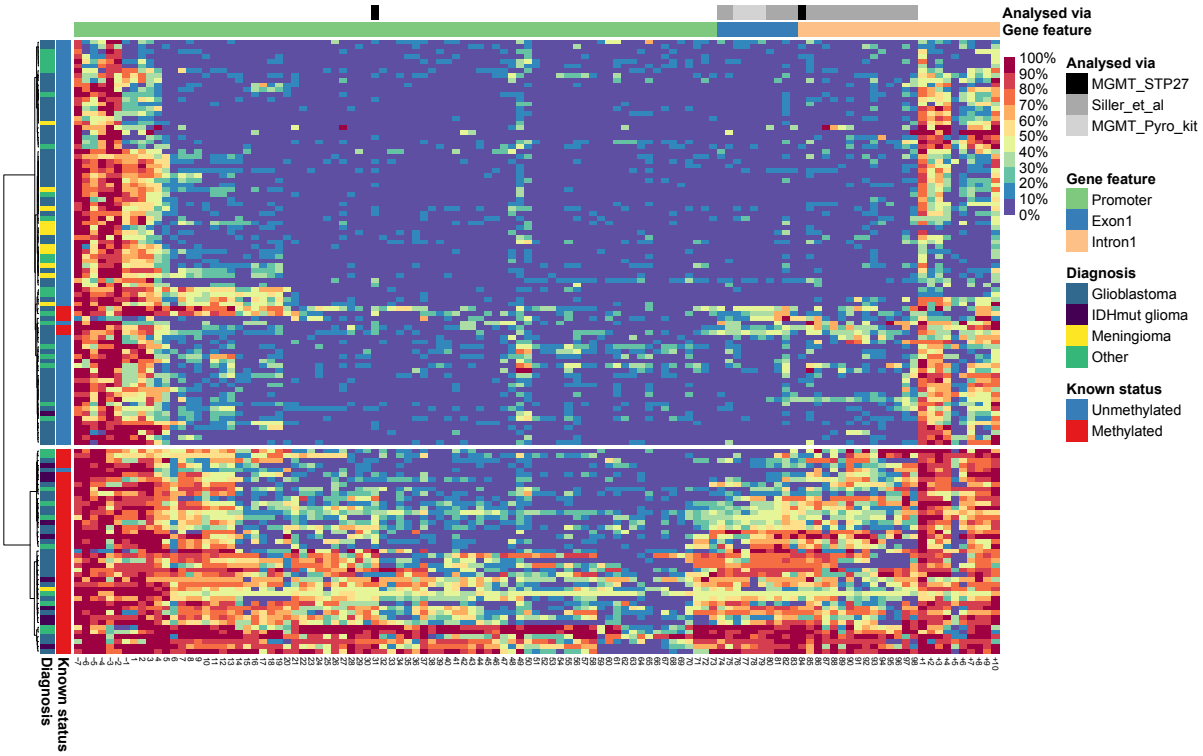

(a)

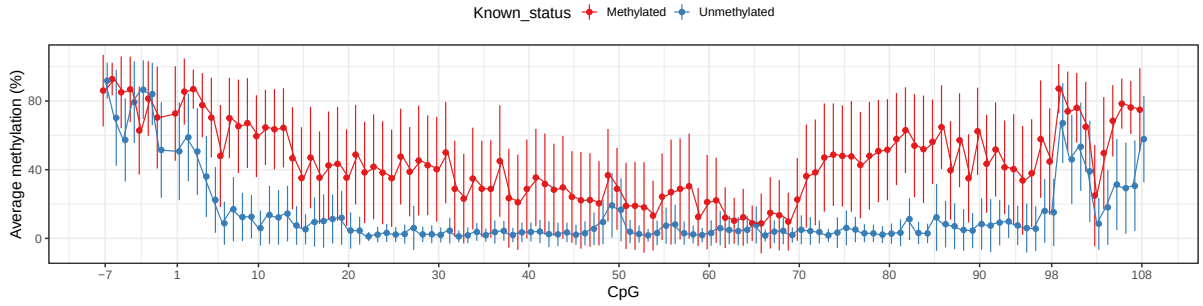

(b)

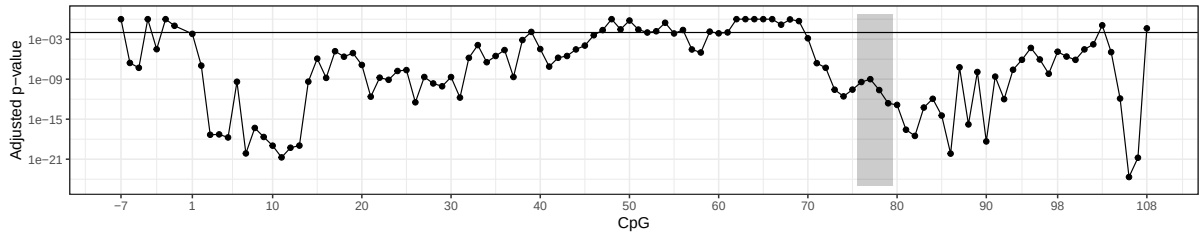

(c)

Figure 5: (a) Unsupervised hierarchical clustering of "prospective nCATs" and "Rapid-CNS" samples based on nanopore sequencing of 117 CpG sites covering the *MGMT* promoter. n = 128. (b) Dotplot showing average methylation percentage of CpG sites in and around the *MGMT* CpG island. Error bars represent standard deviation. (c) Dotplot showing Bonferroni adjusted p-values of Welch's two-sided t-test between methylated and unmethylated samples for every CpG site. Grey vertical bar shows the location of CpG sites analyzed by the MGMT pyro kit. Horizontal line depicts 0.01.

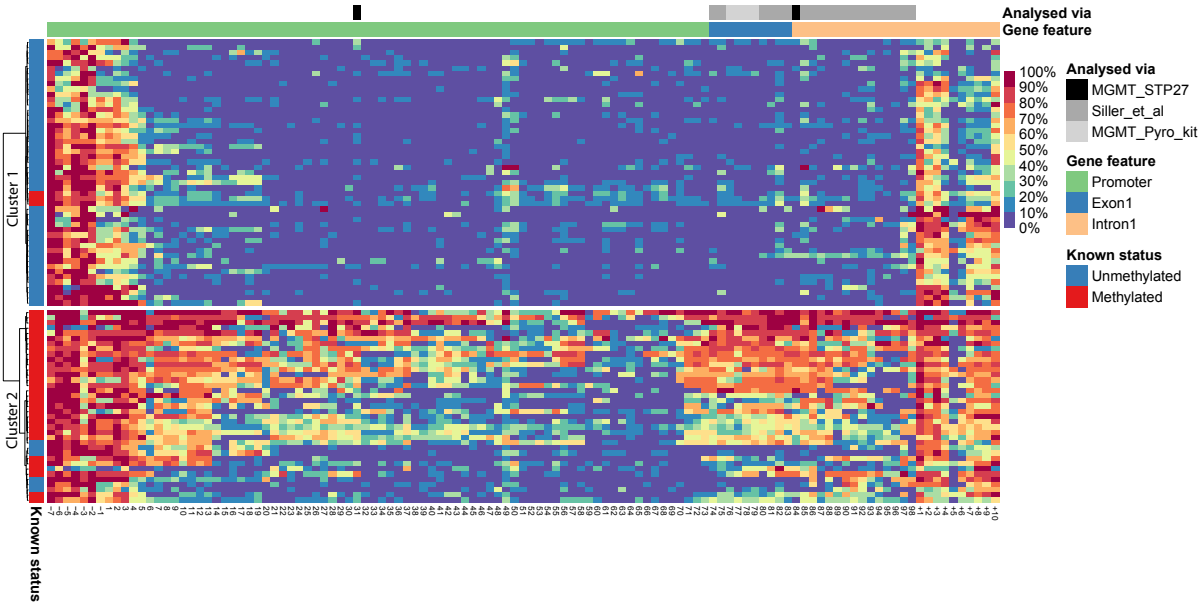

(a)

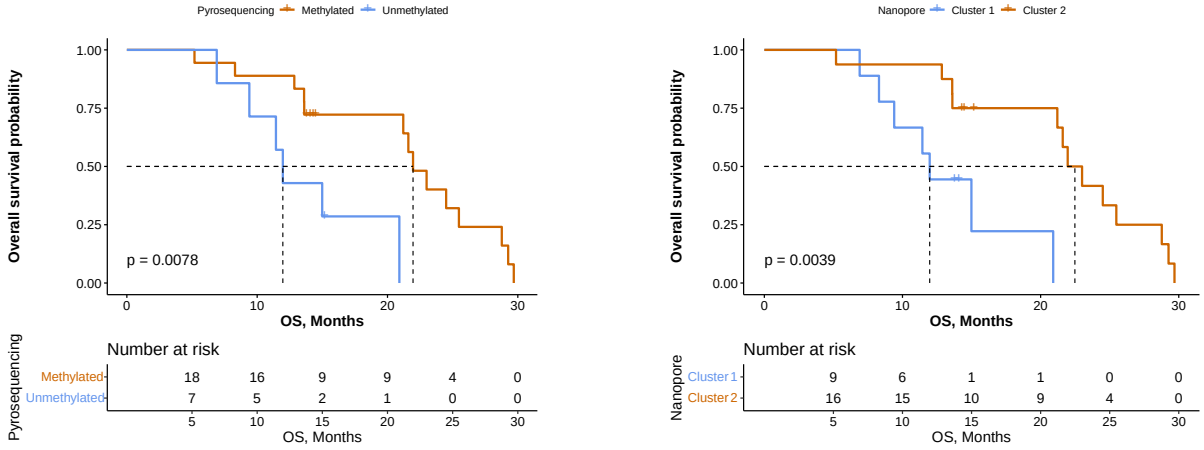

(b)

(c)

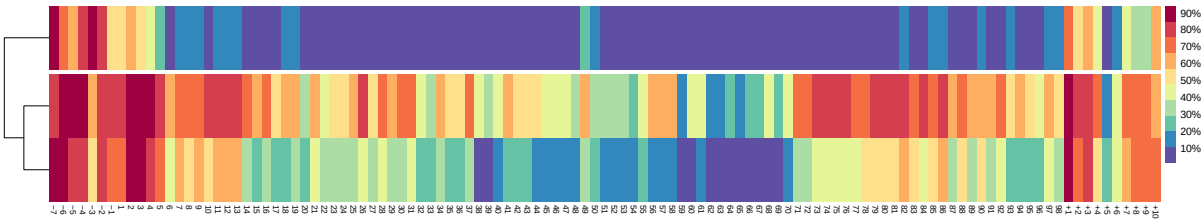

(d)

Figure 6: (a) Heatmap showing unsupervised clustering of all glioblastoma samples based on nanopore sequencing of the *MGMT* promoter (n = 88). Kaplan-Meier patient survival curves based on *MGMT* pyro kit classification (b) or hierarchical clustering according to nanopore sequencing in Figure 6a (c). Dotted lines represent group median survival (Pyrosequencing-methylated = 22.0 months, Pyrosequencing-unmethylated = 12.0 months, Nanopore-Cluster1 = 12.0 months, Nanopore Cluster2 = 22.5 months). d) K-means clustering of glioblastoma samples.

References

[Bady et al., 2016] Bady, P., Delorenzi, M., and Hegi, M. E. (2016). Sensitivity Analysis of the MGMT-STP27 Model and Impact of Genetic and Epigenetic Context to Predict the MGMT Methylation Status in Gliomas and Other Tumors. *Journal of Molecular Diagnostics*, 18(3).

[Bady et al., 2012] Bady, P., Sciuscio, D., Diserens, A. C., Bloch, J., Van Den Bent, M. J., Marosi, C., Dietrich, P. Y., Weller, M., Mariani, L., Heppner, F. L., Mcdonald, D. R., Lacombe, D., Stupp, R., Delorenzi, M., and Hegi, M. E. (2012). MGMT methylation analysis of glioblastoma on the Infinium methylation BeadChip identifies two distinct CpG regions associated with gene silencing and outcome, yielding a prediction model for comparisons across datasets, tumor grades, and CIMP-status. *Acta neuropathologica*, 124(4):547–560.

[Brandner et al., 2021] Brandner, S., McAleenan, A., Kelly, C., Spiga, F., Cheng, H. Y., Dawson, S., Schmidt, L., Faulkner, C. L., Wragg, C., Jefferies, S., Higgins, J. P., and Kurian, K. M. (2021). MGMT promoter methylation testing to predict overall survival in people with glioblastoma treated with temozolomide: A comprehensive meta-analysis based on a Cochrane Systematic Review. *Neuro-Oncology*, 23(9):1457–1469.

[Brigliadori et al., 2016] Brigliadori, G., Foca, F., Dall'Agata, M., Rengucci, C., Melegari, E., Cerasoli, S., Amadori, D., Calistri, D., and Faedi, M. (2016). Defining the cutoff value of MGMT gene promoter methylation and its predictive capacity in glioblastoma. *Journal of Neuro-Oncology*, 128(2).

[Choi et al., 2021] Choi, H. J., Choi, S. H., You, S. H., Yoo, R. E., Kang, K. M., Yun, T. J., Kim, J. H., Sohn, C. H., Park, C. K., and Park, S. H. (2021). MGMT promoter methylation status in initial and recurrent glioblastoma: Correlation study with DWI and DSC PWI features. *American Journal of Neuroradiology*, 42(5).

[Christmann et al., 2011] Christmann, M., Verbeek, B., Roos, W. P., and Kaina, B. (2011). O6-Methylguanine-DNA methyltransferase (MGMT) in normal tissues and tumors: Enzyme activity, promoter methylation and immunohistochemistry. *Biochimica et Biophysica Acta (BBA) - Reviews on Cancer*, 1816(2):179–190.

[Dovek et al., 2019] Dovek, L., Nguyen, N. T., Ozer, B. H., Li, N., Elashoff, R. M., Green, R. M., Liau, L., Leia Nghiemphu, P., Cloughesy, T. F., and Lai, A. (2019). Correlation of commercially avail-

able quantitative MGMT (O-6-methylguanine-DNA methyltransferase) promoter methylation scores and GBM patient survival. *Neuro-Oncology Practice*, 6(3).

[Harris et al., 1991] Harris, L. C., Potter, P. M., Tano, K., Shiota, S., Mitra, S., and Brent, T. P. (1991). Characterization of the promoter region of the human O6-methylguanine-DNA methyltransferase gene. *Nucleic Acids Research*, 19(22).

[Harris et al., 1994] Harris, L. C., Remack, J. S., and Brent, T. P. (1994). Identification of a 59 bp enhancer located at the first exon/intron boundary of the human O6-methylguanine DNA methyltransferease gene. *Nucleic Acids Research*, 22(22).

[Håvik et al., 2012] Håvik, A. B., Brandal, P., Honne, H., Dahlback, H. S. S., Scheie, D., Hektoen, M., Meling, T. R., Helseth, E., Heim, S., Lothe, R. A., and Lind, G. E. (2012). MGMT promoter methylation in gliomas-assessment by pyrosequencing and quantitative methylation-specific PCR. *Journal of Translational Medicine*, 10(1).

[Hegi et al., 2005] Hegi, M. E., Diserens, A.-C., Gorlia, T., Hamou, M.-F., de Tribolet, N., Weller, M., Kros, J. M., Hainfellner, J. A., Mason, W., Mariani, L., Bromberg, J. E., Hau, P., Mirimanoff, R. O., Cairncross, J. G., Janzer, R. C., and Stupp, R. (2005). MGMT Gene Silencing and Benefit from Temozolomide in Glioblastoma . *New England Journal of Medicine*, 352(10).

[Hegi et al., 2019] Hegi, M. E., Genbrugge, E., Gorlia, T., Stupp, R., Gilbert, M. R., Chinot, O. L., Burt Nabors, L., Jones, G., Van Criekinge, W., Straub, J., and Weller, M. (2019). MGMT promoter methylation cutoff with safety margin for selecting glioblastoma patients into trials omitting temozolomide: A pooled analysis of four clinical trials. *Clinical Cancer Research*, 25(6):1809–1816.

[Hegi and Ichimura, 2021] Hegi, M. E. and Ichimura, K. (2021). MGMT testing always worth an emotion. *Neuro-Oncology*, 23(9):1417.

[Huang et al., 2010] Huang, Y., Pastor, W. A., Shen, Y., Tahiliani, M., Liu, D. R., and Rao, A. (2010). The behaviour of 5-hydroxymethylcytosine in bisulfite sequencing. *PLoS ONE*, 5(1).

[Jain et al., 2016] Jain, M., Olsen, H. E., Paten, B., and Akeson, M. (2016). The Oxford Nanopore MinION: Delivery of nanopore sequencing to the genomics community. *Genome Biology*, 17(1).

[Johannessen et al., 2018] Johannessen, L. E., Brandal, P., Myklebust, T. Å., Heim, S., Micci, F., and Panagopoulos, I. (2018). MGMT gene promoter methylation status – Assessment of two pyrosequencing kits and three methylation-specific PCR methods for their predictive capacity in glioblastomas. *Cancer Genomics and Proteomics*, 15(6):437–446.

[Laver et al., 2015] Laver, T., Harrison, J., O'Neill, P. A., Moore, K., Farbos, A., Paszkiewicz, K., and Studholme, D. J. (2015). Assessing the performance of the Oxford Nanopore Technologies MinION. *Biomolecular Detection and Quantification*, 3.

[Malley et al., 2011] Malley, D. S., Hamoudi, R. A., Kocialkowski, S., Pearson, D. M., Collins, V. P., and Ichimura, K. (2011). A distinct region of the MGMT CpG island critical for transcriptional regulation is preferentially methylated in glioblastoma cells and xenografts. *Acta Neuropathologica*, 121(5).

[Nakagawachi et al., 2003] Nakagawachi, T., Soejima, H., Urano, T., Zhao, W., Higashimoto, K., Satoh, Y., Matsukura, S., Kudo, S., Kitajima, Y., Harada, H., Furukawa, K., Matsuzaki, H., Emi, M., Nakabeppu, Y., Miyazaki, K., Sekiguchi, M., and Mukai, T. (2003). Silencing effect of CpG island hypermethylation and histone modifications on O6-methylguanine-DNA methyltransferase (MGMT) gene expression in human cancer. *Oncogene*, 22(55).

[Nguyen et al., 2021] Nguyen, N., Redfield, J., Ballo, M., Michael, M., Sorenson, J., Dibaba, D., Wan, J., Ramos, G. D., and Pandey, M. (2021). Identifying the optimal cutoff point for MGMT promoter methylation status in glioblastoma. *CNS Oncology*, 10(3).

[Ostrom et al., 2020] Ostrom, Q. T., Patil, N., Cioffi, G., Waite, K., Kruchko, C., and Barnholtz-Sloan, J. S. (2020). CBTRUS statistical report: Primary brain and other central nervous system tumors diagnosed in the United States in 2013-2017. *Neuro-Oncology*, 22(Supplement_1):IV1–IV96.

[Patel et al., 2022] Patel, A., Dogan, H., Payne, A., Krause, E., Sievers, P., Schoebe, N., Schrimpf, D., Blume, C., Stichel, D., Holmes, N., Euskirchen, P., Hench, J., Frank, S., Rosenstiel-Goidts, V., Ratliff, M., Etminan, N., Unterberg, A., Dieterich, C., Herold-Mende, C., Pfister, S. M., Wick, W., Loose, M., von Deimling, A., Sill, M., Jones, D. T., Schlesner, M., and Sahm, F. (2022). Rapid-CNS2: rapid comprehensive adaptive nanopore-sequencing of CNS tumors, a proof-of-concept study. *Acta neuropathologica*, 143(5):609–612.

[Payne et al., 2020] Payne, A., Holmes, N., Clarke, T., Munro, R., Debebe, B., and Loose, M. (2020). Nanopore adaptive sequencing for mixed samples, whole exome capture and targeted panels. *bioRxiv*.

[Quillien et al., 2012] Quillien, V., Lavenu, A., Karayan-Tapon, L., Carpentier, C., Labussiäre, M., Lesimple, T., Chinot, O., Wager, M., Honnorat, J., Saikali, S., Fina, F., Sanson, M., and Figarella-Branger, D. (2012). Comparative assessment of 5 methods (methylation-specific polymerase chain reaction, methylight, pyrosequencing, methylation-sensitive high-resolution melting, and immunohistochemistry) to analyze O6-methylguanine-DNA- methyltranferase in a series of 100 glioblastoma patients. *Cancer*, 118(17).

[Radke et al., 2019] Radke, J., Koch, A., Pritsch, F., Schumann, E., Misch, M., Hempt, C., Lenz, K., Löbel, F., Paschereit, F., Heppner, F. L., Vajkoczy, P., Koll, R., and Onken, J. (2019). Predictive MGMT status in a homogeneous cohort of IDH wildtype glioblastoma patients. *Acta neuropathologica communications*, 7(1).

[Siller et al., 2021] Siller, S., Lauseker, M., Karschnia, P., Niyazi, M., Eigenbrod, S., Giese, A., and Tonn, J. C. (2021). The number of methylated CpG sites within the MGMT promoter region linearly correlates with outcome in glioblastoma receiving alkylating agents. *Acta neuropathologica communications*, 9(1):35.

[Stupp et al., 2017] Stupp, R., Taillibert, S., Kanner, A., Read, W., Steinberg, D. M., Lhermitte, B., Toms, S., Idbaih, A., Ahluwalia, M. S., Fink, K., Di Meco, F., Lieberman, F., Zhu, J. J., Stragliotto, G., Tran, D. D., Brem, S., Hottinger, A. F., Kirson, E. D., Lavy-Shahaf, G., Weinberg, U., Kim, C. Y., Paek, S. H., Nicholas, G., Burna, J., Hirte, H., Weller, M., Palti, Y., Hegi, M. E., and Ram, Z. (2017). Effect of tumor-treating fields plus maintenance temozolomide vs maintenance temozolomide alone on survival in patients with glioblastoma a randomized clinical trial. *JAMA - Journal of the American Medical Association*, 318(23).

[Tierling et al., 2022] Tierling, S., Jürgens-Wemheuer, W. M., Leismann, A., Becker-Kettern, J., Scherer, M., Wrede, A., Breuskin, D., Urbschat, S., Sippl, C., Oertel, J., Schulz-Schaeffer, W. J., and Walter, J. (2022). Bisulfite profiling of the MGMT promoter and comparison with routine testing in glioblastoma diagnostics. *Clinical Epigenetics*, 14(1).

[Torre et al., 2022] Torre, M., Wen, P. Y., and Iorgulescu, J. B. (2022). The predictive value of partial MGMT promoter methylation for IDH-wild-type glioblastoma patients . *Neuro-Oncology*

Practice.

[Wenger et al., 2019] Wenger, A., Vega, S. F., Kling, T., Bontell, T. O., Jakola, A. S., and Carén, H. (2019). Intratumor DNA methylation heterogeneity in glioblastoma: implications for DNA methylation-based classification. *Neuro-Oncology*, 21(5):616.

[Wongsurawat et al., 2020] Wongsurawat, T., Jenjaroenpun, P., De Loose, A., Alkam, D., Ussery, D. W., Nookaew, I., Leung, Y. K., Ho, S. M., Day, J. D., and Rodriguez, A. (2020). A novel Cas9-targeted long-read assay for simultaneous detection of IDH1/2 mutations and clinically relevant MGMT methylation in fresh biopsies of diffuse glioma. *Acta Neuropathologica Communications*, 8(1):1–13.

[Xie et al., 2015] Xie, H., Tubbs, R., and Yang, B. (2015). Detection of MGMT promoter methylation in glioblastoma using pyrosequencing. *International Journal of Clinical and Experimental Pathology*, 8(2).

[Yuan et al., 2017] Yuan, G., Niu, L., Zhang, Y., Wang, X., Ma, K., Yin, H., Dai, J., Zhou, W., and Pan, Y. (2017). Defining optimal cutoff value of MGMT promoter methylation by ROC analysis for clinical setting in glioblastoma patients. *Journal of Neuro-Oncology*, 133(1).

[Zhang et al., 2011] Zhang, J., F.G. Stevens, M., and D. Bradshaw, T. (2011). Temozolomide: Mechanisms of Action, Repair and Resistance. *Current Molecular Pharmacology*, 5(1).

Supplementary material

Table 1: Summary of samples included in this study.

	Prospective nCats	Retrospective nCats	Rapid-CNS	Total
Glioblastoma, IDHwt	13	29	49	**91**
Meningioma	0	12	0	**12**
Astrocytoma, HG, IDHmut	0	4	4	**8**
Oligodendroglioma, IDHmut	0	2	6	**8**
Astrocytoma, IDHmut	3	1	3	**7**
Metastasis	0	7	0	**7**
Pilocytic astrocytoma	0	0	4	**4**
Medulloblastoma	0	2	0	**2**
Lymphoma	0	2	0	**2**
Pleomorphic xanthoastrocytoma	0	2	0	**2**
Atypical teratoid/rhabdoid tumor	0	0	1	**1**
CNS Neuroblastoma	0	1	0	**1**
Ependymoma	0	1	0	**1**
Ganglioglioma	0	1	0	**1**
Hemangiopericytoma	0	1	0	**1**
Total	**16**	**65**	**67**	**148**

Table 2: Summary of reported optimal cut-offs for determining methylated versus unmethylated samples

Author	Year	Method	Patients	CpGs	Optimal cut-off	Comment	Reference
Hegi	2019	qMSP	4041		>1.27	"Grey-zone" patients benefit from TMZ	[Hegi et al., 2019]
Johannessen	2018	qMSP, PSQ	48		7 %	PSQ gives better results than other methods	[Johannessen et al., 2018]
Nguyen	2021	PSQ	109		21 %	Higher methylation corrilates with longer OS	[Nguyen et al., 2021]
Quillien	2012	MSP, PSQ, MS-HRM	100	5	8 %	PSQ performs best	[Quillien et al., 2012]
Xie	2015	PSQ	43		10 %	Not testing cut-off	[Xie et al., 2015]
Yuan	2017	PSQ	84	4	12.50 %	Higher methylation corrilates with longer OS	[Yuan et al., 2017]
Brigliadori	2016	PSQ	105	10	30 %	"Grey-zone" patients do not benefit from TMZ	[Brigliadori et al., 2016]
Radke	2019	PSQ, sqMSP	111		10 %	Best results when PSQ and MSP were combined	[Radke et al., 2019]
Chai	2021	PSQ	173	4	10 %	*MGMT* promoter methylation has predictive value in IDH-mutant glioblastoma	[Choi et al., 2021]
Dovek	2019	qMSP	165		>1	"Grey-zone" patients benefit from TMZ, higher methylation does not correlate with longer OS	[Dovek et al., 2019]
Siller	2021	MSP, Sseq	215	25		Linear correlation between number of methylated CpG sites and OS	[Siller et al., 2021]